Journal of Molecular Structure 918 (2009) 14–18

Contents lists available at ScienceDirect

Journal of Molecular Structure

journal homepage: www.elsevier.com/locate/molstruc

Determination of the absolute configuration of two estrogenic nonylphenols in solution by chiroptical methods

Uwe M. Reinscheid *

Max Planck Institute for Biophysical Chemistry, NMR II, Am Fassberg 11, 37 077 Göttingen, Germany

ARTICLE INFO

Article history:
Received 7 April 2008
Received in revised form 9 July 2008
Accepted 10 July 2008
Available online 26 July 2008

Keywords:
Nonylphenol
Absolute configuration
Chiroptical methods
VCD
Optical rotation

ABSTRACT

The absolute configurations of two estrogenic nonylphenols were determined in solution. Both nonylphenols, NP35 and NP112 could not be crystallized so that only solution methods are able to solve directly the question of absolute configuration. The conclusion based on experimental and calculated optical rotation and VCD data for the nonylphenol NP35 was independently confirmed by another study using a camphanoyl derivative and X-ray analysis of the obtained crystals. In case of NP112, the experimental rotation data are inconclusive. However, the comparison between experimental and calculated VCD data allowed the determination of the absolute configuration.

1. Introduction

Nonylphenols (NPs) found in the environment are degradation products of 4-nonylphenol ethoxylates. The latter are non-ionic surfactants with an annual production of 600 000 tons [1]. Due to the chemical production process a variety of isomers is present in the commercial products and consequently in the metabolic nonylphenols. Some of the NPs exhibit estrogenic activities and are therefore of toxicological interest. Theoretically 211 constitutional nonylphenol isomers exist [2]. Many of these isomers possess up to 3 chiral C-atoms, so that in total 550 compounds are possible. Since recent studies have shown that the estrogenic effects of the individual nonylphenol isomers are heavily dependent on the structure of the side alkyl chain [3–6]. It is absolutely necessary to consider nonylphenols from an isomer- and enantiomer-specific viewpoint [2]. More recently, four enantiopure nonylphenol isomers were prepared. Absolute configurations of three isomers have been determined by X-ray crystallographic analysis of the corresponding bromobenzoylated derivatives or camphanoyl derivatives [7,8]. Single-crystal X-ray diffraction (XRD) measurements using anomalous scattering has been the primary tool for determining absolute configurations [9–11]. However, this relatively labor-intensive method requires the availability of crystals of the compound suited for single-crystal X-ray analysis.

In this report, the determination of the absolute configurations of NP35 and NP112 using chiroptical methods, vibrational circular dichroism (VCD) and optical rotation, is presented. Chiroptical techniques are the only methods, except X-ray crystallography, that can determine the absolute configuration of a compound non-empirically. On the other hand, chiroptical methods have the advantage to measure liquid samples. NMR and MS are inherently insensitive to chirality and can only be made sensitive by using auxiliary chiral reagents/media that form diastereomeric complexes.

To date, among the chiroptical data the most familiar were (a) optical rotation [12–14] and (b) electronic circular dichroism (ECD) [15–17]. The electronic transitions of a chiral molecule give rise to circular dichroism (CD) in the visible–ultraviolet (vis–UV) spectral region. Recently, vibrational circular dichroism (VCD) spectroscopy was developed. The relationship between VCD and infrared (IR) absorption is the same as that between ECD and UV absorption. VCD measures the differential absorption of left versus right circularly polarized IR incident light in the molecular vibrational transition. Since its introduction VCD is becoming one of the most powerful and convenient method for the determination of the absolute configuration [18] of natural products, drugs and biomolecules due to the abundance of spectral information delivered by well-resolved peaks in the 1800–1000 cm^{-1} region.

The question of whether a vibrational mode exhibits large VCD or not is ascribed to the magnitude and direction of both electronic- and magnetic-dipole transition moments [19]. Both can be calculated using Gaussian 03 [20].

The instrumental aspects were reviewed already 20 years ago [21] but the computational development lagged behind [19].

* Tel.: +49 551 201 2215; fax: +49 551 201 2202.
E-mail address: urei@nmr.mpibpc.mpg.de

0022-2860/$ - see front matter © 2008 Elsevier B.V. All rights reserved.
doi:10.1016/j.molstruc.2008.07.020

Quantum mechanical predictions of IR and VCD spectra are quite successful in replicating experimental spectra in the mid-IR region. A widely used, reliable theoretical level are DFT calculations with the B3LYP functional and a 6-31G* basis set [22,23]. In some cases, a larger basis set might be necessary but in most instances a satisfactory prediction can be obtained with 6-31G*. The calculated band positions and intensities are used to predict a spectrum typically using Lorentzian band shapes. If the predicted VCD band signs match the corresponding experimentally observed VCD band signs, then the absolute configuration of the molecule is assigned as that used in the calculations. Additionally, the specific optical rotation can be used for the identification of enantiomers. However, valid results need quite large differences between the data for the enantiomers because of the relatively high error associated with the measurement and the calculation procedure.

2. Experimental

Enantiomers of NP35 and NP112 were isolated on a Nucleodex-beta-PM column (5 μm, 250 mm × 10 mm i.d.; Macherey-Nagel, Germany) as reported previously [8,24]. The experimental optical rotations for the nonylphenol isomers were measured on a JASCO P-1030 polarimeter at sodium D line (589 nm).

The infrared and VCD measurements were done with a VERTEX 80 FT-IR spectrometer equipped with a PMA 50 photoeleastic modulator and MCT-Detector (D313/B-A) (Bruker Optics). The IR spectra were recorded with 30 s data collection time at 4 cm^{-1} resolution. The VCD spectra were recorded with 2-hour data collection time at 4 cm^{-1} resolution. All spectra were measured in $CDCl_3$ solvent at a concentration of 10.0 mg/ml (path length 50 μm).

The two isomeric nonylphenols NP35 and NP112 were built using DISCOVER in the InsightII program package (Accelrys™, San Diego, CA). A consistent valence force field (CVFF) force field was chosen. A high temperature (600 K) molecular dynamic/minimization simulation was performed and the resulting energy minimized structures were used as starting structures for Gaussian03™ calculations [20]. The models were geometry optimized using Becke's three parameter hybrid functional in conjunction with the correlation functional of Lee, Yang, and Parr [25–27] and the 6-31G(d) basis set. This level of theory, B3LYP/6-31G(d) for short, was also used for all calculations unless indicated. Frequency calculations were carried out to characterize the optimized structures as energy minima and to obtain the zero-point vibrational energy (ZPVE) corrections. The latter were used unscaled to correct the B3LYP/6-31G(d) energies. Calculations of the infrared, VCD spectra and optical rotation for the different conformers were done using Gaussian03™ [20]. The calculated VCD spectra were frequency-scaled by 0.96 [28,29] and for each enantiomer boltzmann-weighted according to the DFT-calculated Gibbs free energies.

3. Results and discussion

The *R*-configurated two nonylphenol isomers NP35 and NP112 (Figs. 1 and 2) were built in Discover (Accelrys™, San Diego, CA). From the simulated annealing calculations six low-energy conformers were obtained which were used as input structures for the DFT-optimization. The Gibbs free energy at 298.15 K and 1 atm of pressure were calculated by DFT. The lowest-energy conformer was taken as reference, set to 0 kJ/mol, and the resulting energy differences were used to calculate populations according to the Boltzmann distribution. The calculated relative Gibbs free energies of the four lowest-energy conformers of NP35 and NP112 with *R*-configuration are shown in Tables 1 and 2, together with the derived Boltzmann populations. For both isomers, the other conformers were at least 3 kJ/mol higher in energy and therefore neglected. In all conformers the OH group was in the plane of the aromatic ring (Fig. 3) but differed in the orientation indicated by the suffix OH in the name.

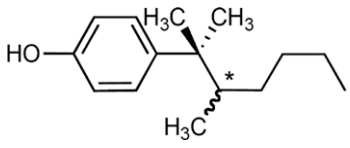

Fig. 1. Formula of NP35.

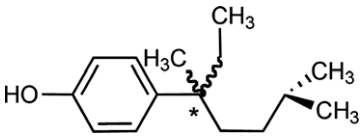

Fig. 2. Formula of NP112.

Table 1
Calculated relative Gibbs free energies, Boltzmann populations and specific optical rotation of the *R*-configurated NP35 conformers

Conformer	Relative Gibbs free energies [kJ/mol]	Population [%]	$[\alpha]_D$
Np35_125	1.52	18.3	+ 45.9
Np35_125_OH	1.73	17.0	+ 18.7
Np35_311	0.25	30.7	+ 86.1
NP35_311_OH	0	34.0	+ 40.6

Table 2
Calculated relative Gibbs free energies, Boltzmann populations and specific optical rotation of the *R*-configurated NP112 conformers

Conformer	Relative Gibbs free energies [kJ/mol]	Population [%]	$[\alpha]_D$
Np112_10	1.43	19.6	−41.5
Np112_10_OH	1.68	17.9	−13.9
Np112_32	0	35.1	+20.4
NP112_32_OH	0.61	27.4	−5.6

The experimental specific rotations of the first elutants of NP35 (designated NP35-E1) and NP112 (designated NP112-E1) were $[\alpha]_D = -27.3$ (c = 1.0, MeOH) and $[\alpha]_D = +0.6$ (*c* = 1.0, MeOH), respectively. The experimental specific rotations of the second elutants of NP35 (designated NP35-E2) and NP112 (designated NP112-E2) are $[\alpha]_D = +24.7$ (*c* = 1.0, MeOH) and $[\alpha]_D = +1.6$ (*c* = 1.0, MeOH), respectively. The boltzmann-weighted specific optical rotation for the *R*-configurated NP35 conformers was calculated at 589 nm ([α]D = +51.8) and compares well with the experimental value of +24.7 for the E2 enantiomer. Thus, based on optical rotation data NP35-E2 is *R*-configurated in agreement with the result for the camphanoyl derivative which was determined independently [24]. The experimental $[\alpha]_D$ value for the E1 enantiomer is −27.3. These values clearly demonstrate the experimental accuracy which can be obtained since there is no inversion of the measured values despite the fact that the two compounds constitute an enantiomeric pair.

The analogous analysis for NP112 failed since there is no inversion of the values again indicating the limit of precision that can be obtained ($[\alpha]_D$ of NP112-E1 = + 0.6 and $[\alpha]_D$ of NP112-E2 = +1.6). The boltzmann-weighted specific optical rotation for the *R*-configurated NP112 conformers was calculated at 589 nm ($[\alpha]_D = -5.0$). Thus, based on optical rotation data the absolute configuration of NP35-E2 cannot be determined conclusively.

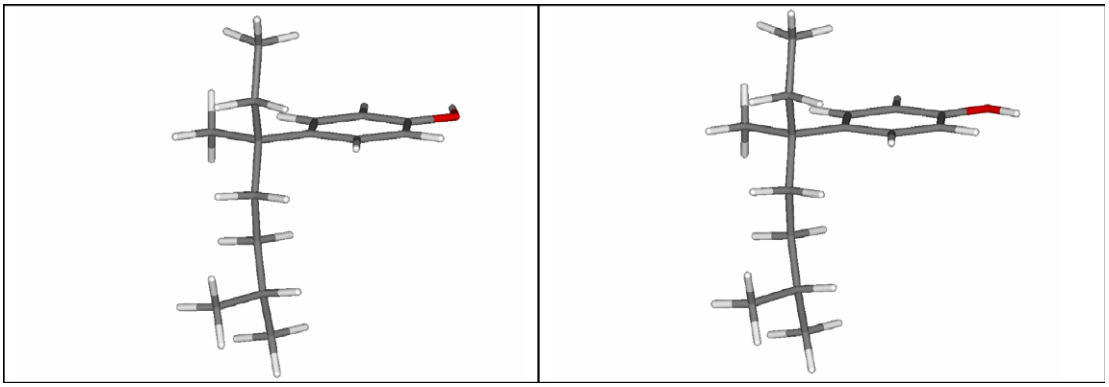

Fig. 3. DFT-optimized conformations of NP112_32 and NP112_32_OH with *R*-configuration.

The Figs. 4 and 5 show the experimental IR and VCD spectra of NP35-E2 and NP112-E1, respectively.

The Figs. 6 and 7 show overlays of the VCD spectra of enantiomeric pairs indicating the absorption bands with discriminating power (marked by an asterisk).

In Fig. 8 the asterisks indicate the discriminating absorption band which can be matched to the boltzmann-weighted calculated VCD spectra of NP35 with *R*-configuration. The enantiomer E2 is therefore *R*-configurated.

Similarly, Fig. 9 shows the overlay between experimental and calculated VCD spectra of NP112. The enantiomer E1 of NP112 is therefore *R*-configurated. Differences are partly due to the averaging procedure for the calculated spectra which is based on DFT-energies *in vacuo*, clearly different from the measurement conditions.

As stated by Bouř et al. [30], the analysis of VCD spectra can be prone to human error. Consequently, in the present investigation the analysis was based on the discriminative bands that were identified by comparison of the two enantiomers. These bands show high intensities of opposite sign and are therefore less prone to errors. The two VCD spectra should be mirror images which is not the case indicating experimental inaccuracies. Nevertheless, the dis-

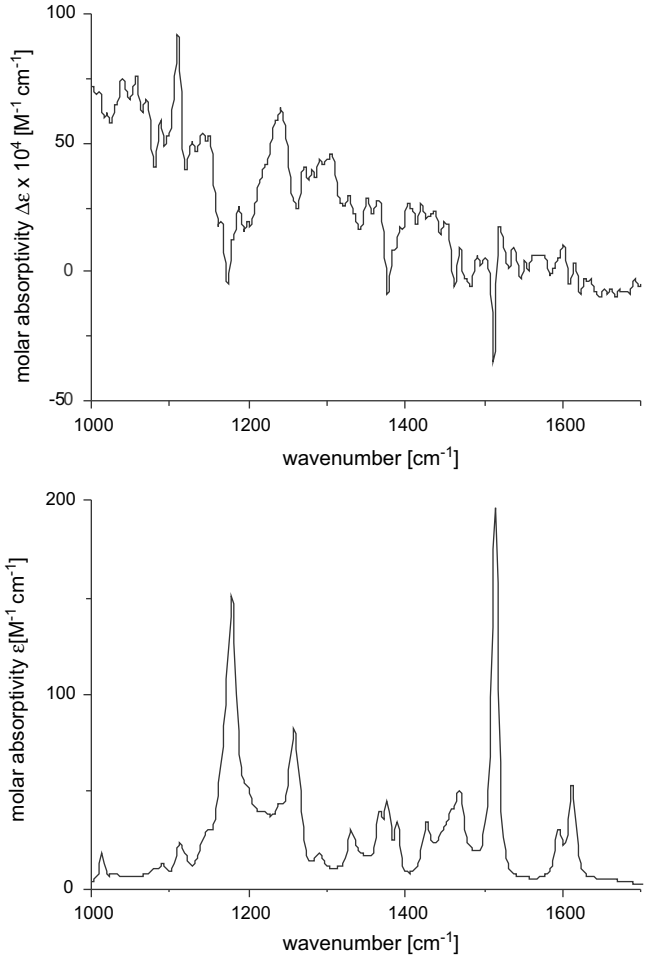

Fig. 4. Experimental IR and VCD spectrum of NP35-E2 in $CDCl_3$.

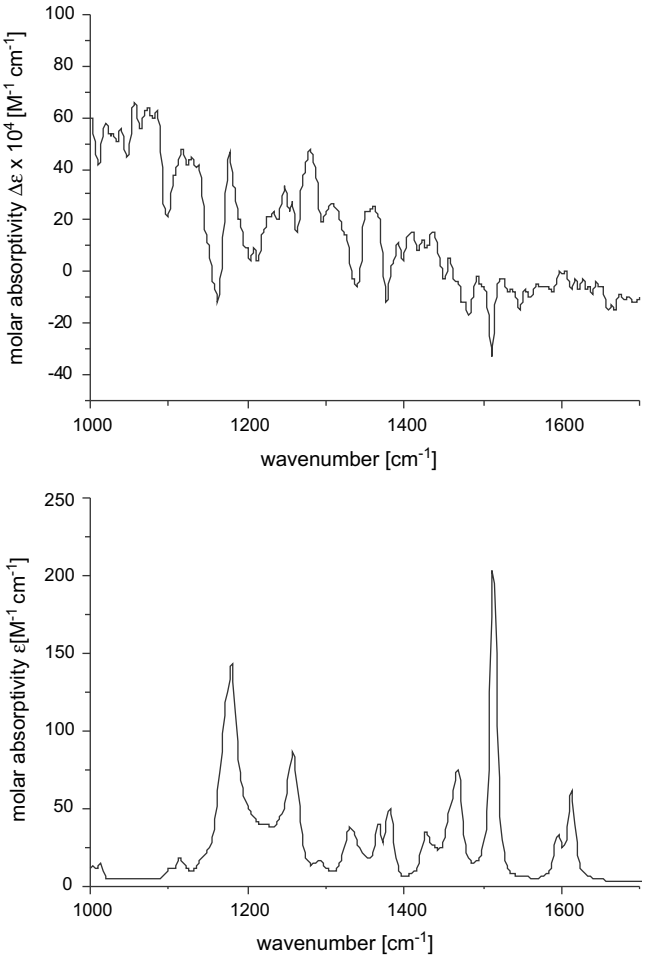

Fig. 5. Experimental IR and VCD spectrum of NP112-E1 in $CDCl_3$.

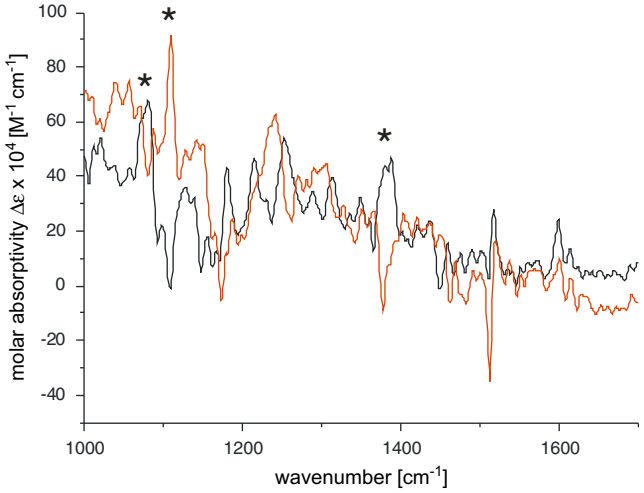

Fig. 6. Experimental VCD spectra of NP35-E1 and E2 in $CDCl_3$ (in black E1, in red E2). (For interpretation of the references to color in this figure legend, the reader is referred to the web version of this article.)

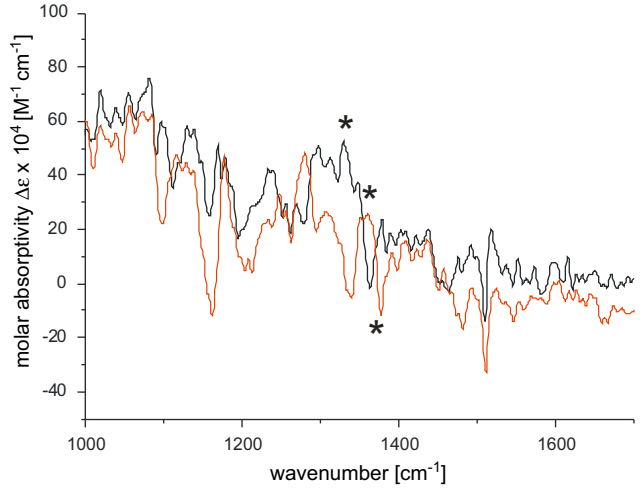

Fig. 7. Experimental VCD spectra of NP112-E1 and E2 in $CDCl_3$ (in red E1, in black E2). (For interpretation of the references to color in this figure legend, the reader is referred to the web version of this article.).

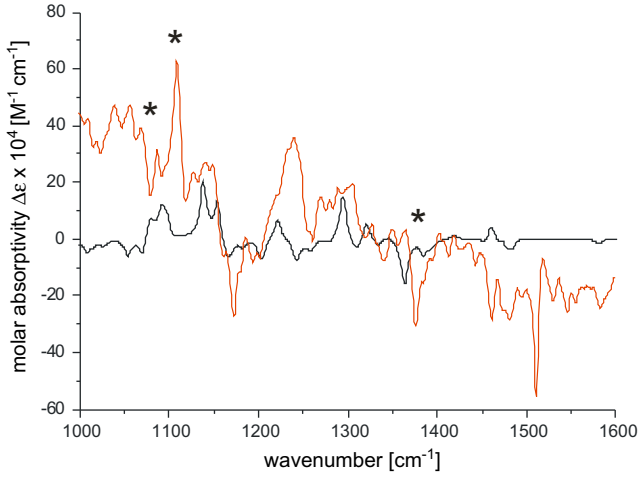

Fig. 8. Comparison between experimental (E2 in red) and calculated (in black) (frequency-scaled by 0.96)(R-configurated) VCD spectra of NP35. (For interpretation of the references to color in this figure legend, the reader is referred to the web version of this article.)

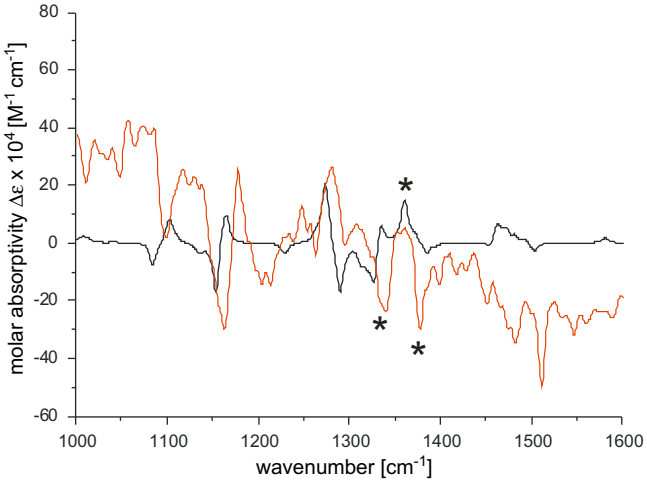

Fig. 9. Comparison between experimental (E1 in red) and calculated (in black) (frequency-scaled by 0.96) (R-configurated) VCD spectra of NP112. (For interpretation of the references to color in this figure legend, the reader is referred to the web version of this article.)

criminative bands allow a clear distinction between the experimental spectra and thereby identify the correct corresponding calculated spectrum.

A number of recent publications show a good match between experimental and calculated VCD spectra. In some cases these results relied on derivatizations [31,32], or on the rigidity of the investigated compounds [33–35].

However, in the case of a phenyl sulphoxide even after scaling of the calculated frequencies a mismatch in peak positions retained [36]. Similarly, the VCD spectrum of a sesquiterpene lactone glycoside needed to be divided into several parts which were scaled independently to obtain a good match between experiment and calculations [37]. In principle, a better match between experimental and calculated VCD spectra could be obtained using matrix isolation VCD (MI-VCD) [38]. However, baseline problems and the dichroism from stressed windows might also lead to some mismatch.

Notoriously problematic are hydrophilic groups such as OH which will form fluctuating H-bond networks not adequately modelled in the calculations. Solvents such as water, deuterium oxide, or DMSO might form hydrogen bonds with the sample molecules and then affect the VCD line shapes, partly by altering the conformation. Derivatization of the OH group can help to improve the match between experimental and calculated VCD spectra as exemplified by Devlin et al. [39] for *endo*-borneol. At the same time, the conformational space was reduced using bulky substituents such as *tert*-butyl. However, to date no routine prediction of the absolute configuration can be achieved for polar compounds in polar solvents. This can be illustrated by two examples. The prediction of the experimental VCD spectrum of camphor-10-sulfonic acid in water was problematic despite inclusion of solvent models [40]. In the case of a piperidine derivative neglecting the solvent contributions to the calculated energies was found not to be relevant for the determination of the absolute configuration since even an equally weighted average yielded the same result [30].

4. Conclusions

In conclusion, the experimental and calculated VCD spectra of the two nonylphenols in this study show no 1:1 correspondence. However, with the restriction to discriminative bands, the absolute configurations can be determined unambiguously by VCD. For

NP35 optical rotation data support the assignment whereas for NP112 the experimental data prohibit reliable predictions.

Acknowledgements

I thank H. Zhang and Prof. Spiteller (Dortmund, Germany), and Dr. Drews (BrukerOptics, Ettlingen, Germany).

References

[1] C.D. Hager, in: D.R. Karsa (Ed.), Annual Surfactant Review, Sheffield Academic Press, Sheffield, 1998, p. 1.
[2] K. Guenther, E. Kleist, B. Thiele, Anal. Bioanal. Chem. 384 (2006) 542.
[3] N. Yamashita, K. Kannan, S. Hashimoto, A. Miyazaki, J.P. Giesy, Organohalogen Compd. 42 (1999) 121.
[4] K. Guenther, V. Heinke, B. Thiele, E. Kleist, H. Prast, T. Raecker, Environ. Sci. Technol. 37 (2003) 2624.
[5] Y.S. Kim, T. Katase, Y. Horii, N. Yamashita, M. Makino, T. Uchiyama, Y. Fujimoto, T. Inoue, Jpn. Mar. Pollut. Bull. 51 (2005) 850.
[6] Y.S. Kim, T. Katase, S. Sekine, T. Inoue, M. Makino, T. Uchiyama, Y. Fujimoto, N. Yamashita, Chemosphere 54 (2004) 1127.
[7] H. Saito, T. Uchiyama, M. Makino, T. Katase, Y. Fujimoto, D. Hashizume, J. Health Sci. 53 (2007) 177.
[8] H. Zhang, I.M. Oppel, M. Spiteller, K. Guenther, G. Boehmler, S. Zuehlke, Chirality, 2008, in press, doi:10.1002/chir.20556.
[9] J.M. Bijvoet, A.F. Peerdeman, A.J. van Bommel, Nature 168 (1951) 271.
[10] H.D. Flack, G. Bernardinelli, Acta Crystallogr. A 55 (1999) 908.
[11] H.D. Flack, G. Bernardinelli, J. Appl. Crystallogr. 33 (2000) 1143.
[12] P.J. Stephens, D.M. McCann, J.R. Cheeseman, M.J. Frisch, J. Phys. Chem. A 105 (2001) 5356.
[13] P.J. Stephens, F.J. Devlin, J.R. Cheeseman, M.J. Frisch, Chirality 17 (2005) S52.
[14] P.L. Polavarapu, D.K. Chakraborty, Chem. Phys. 240 (1999) 1.
[15] K.M. Specht, J. Nam, D.M. Ho, N. Berova, R.K. Kondru, D.N. Beratan, P. Wipf, R.A. Pascal, D. Kahne, J. Am. Chem. Soc. 123 (2001) 8961.
[16] G. Uray, P. Verdino, F. Belaj, C.O. Kappe, W.M.F. Fabian, J. Org. Chem. 66 (2001) 6685.
[17] G. Pesciteli, S. Gabriel, Y.K. Wang, J. Fleischhauer, R.W. Woody, N. Berova, J. Am. Chem. Soc. 125 (2003) 7613.
[18] T.B. Freedman, X. Cao, R.D. Dukor, L.A. Nafie, Chirality 15 (2003) 743; T. Kuppens, P. Bultinck, W. Langenaeker, Drug Discov. Today: Technol. 1 (2004) 269.
[19] L.A. Nafie, Annu. Rev. Phys. Chem. 48 (1997) 357.
[20] M.J. Frisch, et al., Gaussian 03, Revision B.02, Gaussian, Inc., 2003.
[21] P.J. Stephens, M.A. Lowe, Annu. Rev. Phys. Chem. 36 (1985) 213.
[22] J.R. Cheeseman, M.J. Frisch, F.J. Devlin, P.J. Stephens, Chem. Phys. Lett. 252 (1996) 211.
[23] P.J. Stephens, F.J. Devlin, Chirality 12 (2000) 179.
[24] H. Zhang, S. Zühlke, K. Günther, M. Spiteller, Chemosphere 66 (2007) 594.
[25] C. Lee, W. Yang, R.G. Parr, Phys. Rev. B 37 (1988) 785.
[26] A.D. Becke, J. Chem. Phys. 98 (1993) 5648.
[27] P.J. Stephens, F.J. Devlin, C.F. Chabalowski, M.J. Frisch, J. Phys. Chem. 98 (1994) 11623.
[28] P.S. Anthony, R. Leo, J. Phys. Chem. 100 (1996) 16502.
[29] M.W. Wong, Chem. Phys. Lett. 256 (1996) 391.
[30] P. Bouř, H. Navrátilová, V. Setnička, M. Urbanová, K. Volka, J. Org. Chem. 67 (2002) 161.
[31] K. Krohn, D. Gehle, S.K. Dey, N. Nahar, M. Mosihuzzaman, N. Sultana, M.H. Sohrab, P.J. Stephens, J.-J. Pan, F. Sasse, J. Nat. Prod. 70 (2007) 1339.
[32] F.J. Devlin, P.J. Stephens, P. Besse, Tetrahedron: Asymmetry 16 (2005) 1557.
[33] T. Kuppens, K. Vandyck, J. Van der Eycken, W. Herrebout, B.J. Van der Veken, P. Bultinck, J. Org. Chem. 70 (2005) 9103.
[34] E. Tur, G. Vives, G. Rapente, J. Crassous, N. Vanthuyne, C. Roussel, R. Lombardi, T. Freedman, L. Nafie, Tetrahedron: Asymmetry 18 (2007) 1911.
[35] H.M. Min, M. Aye, T. Taniguchi, N. Miura, K. Monde, K. Ohzawa, T. Nikai, M. Niwa, Y. Takaya, Tetrahedron Lett. 48 (2007) 6155.
[36] A.G. Petrovic, J. He, P.L. Polavarapu, L.S. Xiao, D.W. Armstrong, Org. Biomol. Chem. 3 (2005) 1977.
[37] O. Michalski, W. Kisiel, K. Michalska, V. Setnička, M. Urbanová, J. Mol. Struct. 871 (2007) 67.
[38] G. Tarczay, G. Magyarfalvi, E. Vass, Angew. Chem. Int. Ed. 45 (2006) 1775.
[39] F.J. Devlin, P.J. Stephens, P. Besse, J. Org. Chem. 70 (2005) 2980.
[40] H.E. Morita, T.S. Kodama, T. Tanaka, Chirality 18 (2006) 783.